PRAMANA — journal of physics
© Indian Academy of Sciences
Vol. 70, No. 4
April 2008
pp. 679–696

Electron density distribution in Si and Ge using multipole, maximum entropy method and pair distribution function analysis

R SARAVANAN[1,*], K S SYED ALI[2] and S ISRAEL[3]
[1]Department of Physics, The Madura College, Madurai 625 011, India
[2]Department of Physics, Yadava College, Madurai 625 014, India
[3]Department of Physics, The American College, Madurai 625 002, India
*Corresponding author. E-mail: saragow@dataone.in

MS received 29 April 2007; revised 18 September 2007; accepted 17 October 2007

Abstract. The local, average and electronic structure of the semiconducting materials Si and Ge has been studied using multipole, maximum entropy method (MEM) and pair distribution function (PDF) analyses, using X-ray powder data. The covalent nature of bonding and the interaction between the atoms are clearly revealed by the two-dimensional MEM maps plotted on (1 0 0) and (1 1 0) planes and one-dimensional density along [1 0 0], [1 1 0] and [1 1 1] directions. The mid-bond electron densities between the atoms are 0.554 e/Å^3 and 0.187 e/Å^3 for Si and Ge respectively. In this work, the local structural information has also been obtained by analyzing the atomic pair distribution function. An attempt has been made in the present work to utilize the X-ray powder data sets to refine the structure and electron density distribution using the currently available versatile methods, MEM, multipole analysis and determination of pair distribution function for these two systems.

Keywords. Electron density; Si; Ge; X-ray powder data; maximum entropy method; multipole analysis; pair distribution function.

PACS Nos 61.00; 61.10.Nz; 61.10.-i

1. Introduction

To understand the nature of the chemical bonds precisely, an accurate electron density distribution is indispensable. To date, there have been many studies on the electron densities for Si and Ge both experimentally and theoretically because of their importance as semiconductors, e.g., for Si, Lu and Zunger [1] compared the measured electron density distribution with *ab initio* theoretical calculations within the local density formalism; Deutsch [2] used the multipole expansion for analysing the data of Si; Spackman [3,4] derived deformation and valance electron density via Fourier summation and used the multipole refinement for Si and

diamond; Sakata and Sato [5] evolved the precise electron density of Si by maximum entropy method. For Si and Ge, Deutsch *et al* [6] have studied theoretically and experimentally the charge density. The precise electron density distribution by maximum entropy method, with limited number of structure factors has been studied for many materials, for e.g., [7–14]. The determination of pair distribution function is a tool for understanding the local structure of materials. Proffen and Billinge [15] studied Cu_3Au for the chemical short-range order obtained from the atomic pair distribution function. Egami [16] has studied the atomic correlations in non-periodic matter for aluminum and the superconducting material $TiBa_2CaCu_2O_8$. In the present analysis, the two systems Si and Ge have been analyzed in the lines of atomic pair distribution functions also using X-ray powder data. The present work can be considered to be the first attempt to study two important semiconductors using X-ray powder data and the versatile tools like multipole, MEM and pair distribution function.

2. Theory

2.1 *Multipole analysis*

Hansen and Coppens [17] proposed a modified electron density model with the option that allows the refinement of population parameters at various orbital levels where the atomic density is described as a series expansion in real spherical harmonic functions through fourth-order Y_{lm}. According to this model, the charge density in a crystal is defined as the superposition of harmonically vibrating aspherical atomic density distribution convolving with the Gaussian thermal displacement distribution as

$$\rho(r) = \sum_{k}^{\text{atoms}} \rho_k(\vec{r} - \vec{r}_k - \vec{u}\,) \otimes t_k(\vec{u}\,), \tag{1}$$

where $t_k(\vec{u}\,)$ is the Gaussian term and $\otimes$ indicates a convolution. The atomic charge density is then defined as

$$\begin{aligned}\rho(\vec{r}\,) = {} & P_c\rho_{\text{core}}(\bar{r}) + P_v\kappa'^3\rho_{\text{valence}}(\kappa' r) \\ & + \sum_{l=0}^{4} \kappa''^3 R_l(\kappa'' r) \sum_{m=-l}^{l} P_{lm} Y_{lm}(\vec{r}/r),\end{aligned} \tag{2}$$

where P_c, P_v and P_{lm} are population coefficients. Canonical Hartree–Fock atomic orbitals of the free atoms normalized to one electron can be used for the construction of ρ_{core} and ρ_{valence}, but the valence function is allowed to expand and contract by the adjustment of the variable parameters κ' and κ''. The effect of the temperature can be distinguished from the convoluted and the deconvoluted forms of thermal contribution to the charge density as dynamic and static multipole deformation maps. The deformation density in these maps are characterized by

$$\Delta\rho_{\text{multipole-deformation}}(\vec{r}\,) = \frac{1}{V}\sum[F(\vec{h})_{\text{multipole}} - F(\vec{h})_{\text{spherical-atom}}]\exp[-2\pi i(\vec{h}\cdot\vec{r}\,)], \qquad (3)$$

where $F_{\text{multipole}}$ is the Fourier transform of the multipole charge density with or without the convolution of thermal contribution, where the Fourier components are terminated at the experiment resolution.

Several results for MEM analysis have been given in our earlier papers, i.e., [7,8,11–13,18]. A brief theory on MEM has been given in the next section.

2.2 *Maximum entropy method (MEM)*

The MEM is an exact tool to study the electron density distribution because of its resolution. When compared with the conventional Fourier synthesis the MEM is more informative. In Fourier synthesis, the electron densities will be biased, due to the series termination error, and negative electron density that prevents clear understanding of bonding between the atoms. But MEM analysis overcomes these problems.

The exact electron density distribution would be obtained if all the structure factors were known without any ambiguities. It is however, impossible to collect exact values of all the structure factors by X-ray diffraction methods. The number of observed structure factors by the experiment is limited and have some errors in them. From the viewpoint of the information theory, it is not appropriate to use an inverse Fourier transform to construct density distribution by using such a limited number of observed structure factors. The maximum entropy method (MEM) is one of the appropriate methods in which the concept of entropy is introduced to handle the uncertainty properly. The principle of MEM is to obtain an electron density distribution which is consistent with the observed structure factors and to leave the uncertainties maximum.

The MEM is a method to derive the most probable electron density map given a set of experimental data. It is a model-free approach in contrast to structure refinements in which the positions of spherical atoms are determined. Therefore, the MEM is most suited to study aspects of structures that go beyond the independent atom approximation, like partially ordered structures, the electron density in the chemical bond, and the effects of anharmonic atomic vibrations.

The precise study of the bonding in materials is always useful and interesting. Yet no study can reveal the real picture, because no two experimental data are identical. This problem turns out to be enhanced when the model used for the evaluation of electron densities is not completely suitable. The bonding nature and the distribution of electrons in the bonding region can be clearly visualized using this technique. MEM electron densities are always positive and even with limited number of data one can evaluate reliable electron densities resembling true densities.

MEM is introduced in radio astronomical image processing. The maximum entropy method gives actual electron density rather than a normalized one. No phase information is needed for MEM calculations. It leads to least biased calculations. It performs accurately even with limited information [11].

Collin's [19] formalism is based on the entropy expression S, given by

$$S = -\sum \rho'(r) \ln \frac{\rho'(r)}{\tau'(r)}, \tag{4}$$

where $\rho(r)$ is the electron density at a certain pixel r and $\tau'(r)$ is the prior density for $\rho(r)$. We introduce the constraint as

$$C = \frac{1}{N} \frac{\sum |F_{\mathrm{cal}}(K) - F_{\mathrm{obs}}(K)|^2}{\sigma^2(F_{\mathrm{obs}}(K))}, \tag{5}$$

where N is the number of reflections, $\sigma(k)$ is the standard deviation of $F_{\mathrm{obs}}(K)$ and V is the unit cell volume

$$F_{\mathrm{cal}}(K) = V \sum \rho(r) \exp(2\pi i k \cdot r) \mathrm{d}v. \tag{6}$$

The expected value for C is 1. We use the Lagrange's method of undetermined multiplier to constrain C to be unity while we maximize the entropy. Then we have

$$Q(\lambda) = -\sum \rho(r) \ln \frac{\rho(r)}{\tau(r)} \frac{\lambda C}{2}. \tag{7}$$

By setting $\frac{\mathrm{d}Q(\lambda)}{\mathrm{d}\rho(r)} = 0$ and solving for $\rho(r)$ using approximation $\ln(X) = X - 1$

$$\rho(r) = \exp\left[\frac{\ln \tau(r) + \lambda F_{\mathrm{cal}}(0)}{N} \frac{\sum (F_{\mathrm{obs}}(K) - F_{\mathrm{cal}}(K)) \exp(-i2\pi i k \cdot r)}{\sigma^2(K)}\right]. \tag{8}$$

This is refined until $C = 1$, the final result is

$$\rho(r) = \rho_{\mathrm{MEM}}(r). \tag{9}$$

2.3 *Pair distribution function*

For materials which lack long-range order, or where short-range order structure is not reflected in the long-range order of the crystal, an alternate structural analysis approach is used. In this method, sometime called the real-space structure determination method, the pair distribution function (PDF) is modeled in real space, rather than in the reciprocal space. The PDF reflects the short-range ordering in a material. This approach has been widely used for studying the structure of materials, glasses and liquids [20–22]. More recently, it has been applied to disordered crystalline and partially crystallized materials. Quantitative structural information on nanometer length scales can be obtained by fitting a model directly to the PDF [23–25].

The PDF method shows that when there are no short-range deviations from the average structure, the PDF agrees well with the inter-atomic distances computed from a crystallographic model [26,27].

This real space method is one of a very small number of experimental techniques that can be used to probe the structure on the nanometer length scale, when the local structure is not consistent with the long-range, globally averaged structure [28].

The scattered X-ray intensity by a collection of atoms can be expressed as follows: (after corrections for absorption, polarization, multiple scattering and normalization to the unit of one atom or scattering),

$$I(Q) = \sum_{i,j} f_i(\vec{Q}) f_j(\vec{Q}) \langle\langle \exp(i\vec{Q} \cdot (r_i - r_j)) \rangle\rangle, \tag{10}$$

where $f_j(Q)$ is the scattering amplitude of single atom i, r_i is the position, $\vec{Q}$ is the scattering vector and $\langle\langle \exp(i\vec{Q} \cdot (r_i - r_j)) \rangle\rangle$ is the quantum and thermal average Q is given by

$$\vec{Q} = K_f - K_i, \tag{11}$$

$$Q = |\vec{Q}| = 2|K_{f,i} \sin\theta \quad \text{if } K_f = K_i. \tag{12}$$

Here K_f and K_i are the momenta of scattered and incident X-ray photons respectively and θ is the diffraction angle. The quasi-elastic X-ray scattering includes inelastic phonons scattering too.

The average structure factor can be given as

$$S(\vec{Q}) = \frac{I(\vec{Q})}{\langle f(\vec{Q}) \rangle^2} + \frac{[\langle f(\vec{Q}) \rangle^2 - \langle f(\vec{Q})^2 \rangle]}{\langle f(\vec{Q}) \rangle^2}. \tag{13}$$

Here $\langle f(\vec{Q}) \rangle^2$ is the compositional average. This equation for $S(\vec{Q})$ can be noted as the square of the structure factor $F(\vec{Q})$.

Instead of indexing and analyzing each peak separately, the total data will be treated in real space, by Fourier transforming the data. The Fourier transform of eq. (13) in 3D gives the atomic pair distribution function.

$$\rho(r) = \rho_0 + \frac{1}{2\pi^2 r} \int \vec{Q}[S(\vec{Q}) - 1] \sin(\vec{Q}r) \mathrm{d}\vec{Q}, \tag{14}$$

where ρ_0 = average (atomic) number density (average no. of atoms in the sample with respect to distance) and r = distance.

If $\vec{Q}$ is in Å^{-1}, then $\rho(r)$ will be in Å^{-3}. $\rho(r)$ corresponds to the (atomic) number density at a distance r from the average atom. Equation (14) is expressed as follows:

$$[\rho(r) - \rho_0] = \frac{1}{2\pi^2 r} \int \vec{Q}[S(\vec{Q}) - 1] \sin(\vec{Q}r) \mathrm{d}\vec{Q}, \tag{15}$$

$$4\pi r[\rho(r) - \rho_0] = \frac{4\pi r}{2\pi^2 r} \int \vec{Q}[S(\vec{Q}) - 1] \sin(\vec{Q}r) \mathrm{d}\vec{Q}, \quad (16)$$

$$G(r) = 4\pi r[\rho(r) - \rho_0] = \frac{2}{\pi} \int \vec{Q}[S(\vec{Q}) - 1] \sin(\vec{Q}r) \mathrm{d}\vec{Q}. \quad (17)$$

$G(r)$ will be in units of Å^{-2} if $\vec{Q}$ is in Å^{-1} [16].

In the present work, the powder X-ray data of Si and Ge have been utilized for the analysis of pair distribution function. The observed PDF's have been obtained from the software package PDFGetX [29]. The PDF for Si and Ge were refined using PDFFIT [24]. Then the observed and calculated PDF's have been compared and analyzed. The atomic pair distribution function can be obtained from powder diffraction data and is a valuable tool for the study of the local atomic arrangements in a material. The determination of the crystal structure is an important part in crystallography, and the structure deformation studies are based on the analysis of the intensities and positions of Bragg reflections which only allows one to determine the long-range average structure [30]. The Bragg and diffuse scattering information about local arrangements is preserved in PDF. The PDF can be understood as a bond-length distribution between all pairs of atoms within the crystal (up to the maximum distance); however, each contribution has a weight corresponding to the scattering power of the two atoms involved. The analysis of Bragg scattering assumes a perfect long-range periodicity of the crystal. However, many materials are quite disordered and even more important, the key to the deeper understanding of their properties is the study of deviations from the average structure or the study of the local atomic arrangements [31].

3. Experiment

The very high quality Si and Ge single crystal samples were ground into fine powders using mortar pestle and sieved using 400 mesh nylon cloth. The powder X-ray data were collected using X'PERT PRO (Philips, The Netherlands) X-ray diffractometer. The wavelength used for X-ray intensity data collection is 1.54056 Å. The 2θ range of data collection was 10°–120° and 10°–90° for Si and Ge respectively. The step size of the data sets is 0.05 for both Si and Ge.

4. Data analysis

The Rietveld [32] full profile analysis is the standard tool for analysis of crystalline sample made into powders. In this technique, structural parameters, lattice parameters, peak shift, background profile shape and preferred orientation must be refined in addition to scale factor and other allowed parameters. The two data sets have been analyzed using the Rietveld-type software package JANA 2000 [33] that has provisions for refinement based on multipole formalism. The refined and matched intensity profiles for Si and Ge are shown in figures 1a and 1b. The refined F_{obs}, F_{cal} values are tabulated in tables 1 and 2 for Si and Ge respectively. The

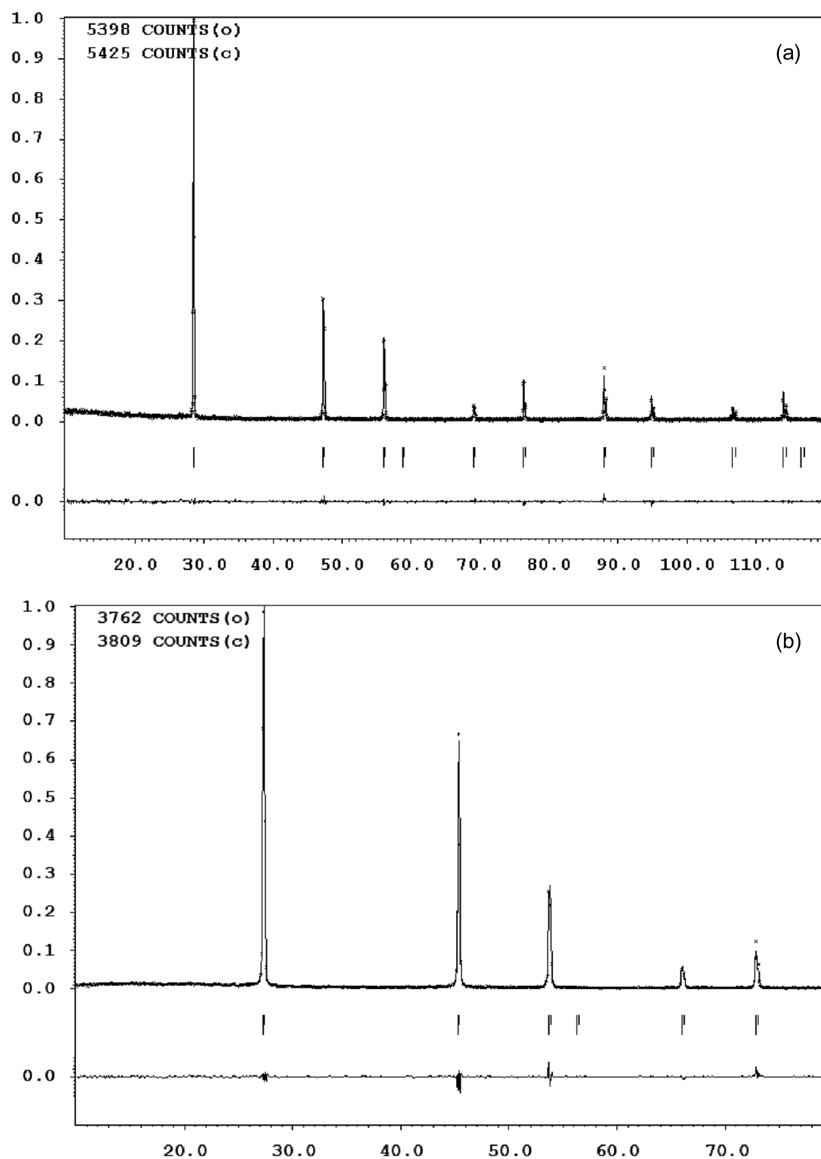

Figure 1. (**a**) The Rietveld refinement/powder profile of Si. (**b**) The Rietveld refinement/powder profile of Ge.

refined cell parameters of the unit cells are 5.4328 (0.1840) Å, 5.6664 (0.1764) Å Si and Ge respectively. The cell parameters in this work are in close agreement with the reported values 5.4307 Å and 5.6573 Å [34]. The electron densities from multipole analysis have been shown in figures 2a and 2b as dynamic multipole deformation maps (DMD) on the (1 0 0) plane of Si and Ge respectively. Figures 3a and 3b represent the static multipole deformation maps (SMD) on (1 0 0) plane

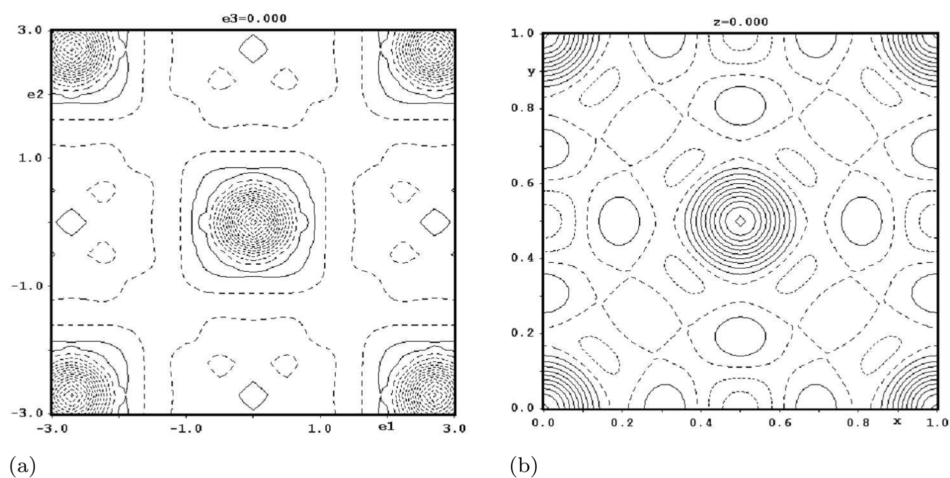

(a) (b)

Figure 2. Dynamic multipole deformation map of (**a**) Si on (1 0 0) plane and (**b**) Ge on (1 0 0) plane.

Table 1. Observed and calculated structure factors for Si refined using JANA 2000.

h k l	F_{obs}	F_{cal}	$F_{\text{obs}} - F_{\text{cal}}$	$\sigma(F_{\text{obs}})$
1 1 1	60.09	60.16	−0.07	0.10
2 0 2	69.23	68.96	0.27	0.22
1 1 3	44.31	45.05	−0.73	0.73
0 0 4	58.60	57.31	1.28	0.61
3 1 3	36.99	38.36	−1.36	0.96
2 2 4	52.21	49.51	2.70	1.14
3 3 3	30.63	33.19	−2.56	1.02
1 1 5	30.62	33.18	−2.56	1.02
4 0 4	41.67	43.02	−1.34	1.58
3 1 5	28.91	28.90	0.01	0.75

Table 2. Observed and calculated structure factors for Ge refined using JANA 2000.

h k l	F_{obs}	F_{cal}	$F_{\text{obs}} - F_{\text{cal}}$	$\sigma(F_{\text{obs}})$
1 1 1	147.05	147.37	−0.31	1.15
2 0 2	173.90	173.75	0.14	1.73
1 1 3	116.37	114.53	1.84	1.50
0 0 4	146.89	145.88	1.00	4.28
3 1 3	93.95	95.70	−1.71	1.96

Table 3. Parameters from multipole refinement.

Parameter	Si	Ge
P_c	10	28
P_v	4	4
κ'	0.98	1.022(0.047)
κ''	1.00	1.153(0.251)
P_{40}	0.0652	1.0493
P_{44}	0.0483	0.7769
B	0.5858	0.5680
B	0.4819*	0.5938*
B	0.4510***	0.5280**
GoF	1.13	1.05
R (%)	2.85	0.75
wR (%)	0.79	0.83

*Theoretical [39]; **Experimental [40]; ***Experimental [41].

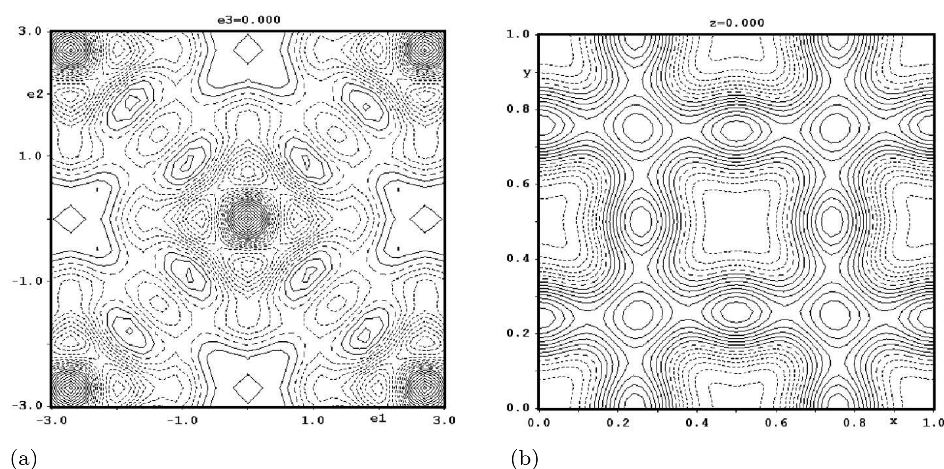

Figure 3. Static multipole deformation map of (**a**) Si on (1 0 0) plane and (**b**) Ge on (1 0 0) plane.

of Si and Ge respectively. Figures 4a and 4b are dynamic multipole deformation maps (DMD) on (1 1 0) plane of Si and Ge respectively. Figures 5a and 5b represent the static multipole deformation maps (SMD) on (1 1 0) plane of Si and Ge respectively. The results of the multipole refinement are given in table 3, which shows the multipole parameters, κ' and κ'', the reliability indices R and wR. The results of the electron densities from multipole analysis are given in table 4. The refined multipole structure factors were used for the MEM refinements of the electron densities. To analyse the MEM results, one-dimensional profiles along different directions of the unit cell and two-dimensional electron density contour maps have

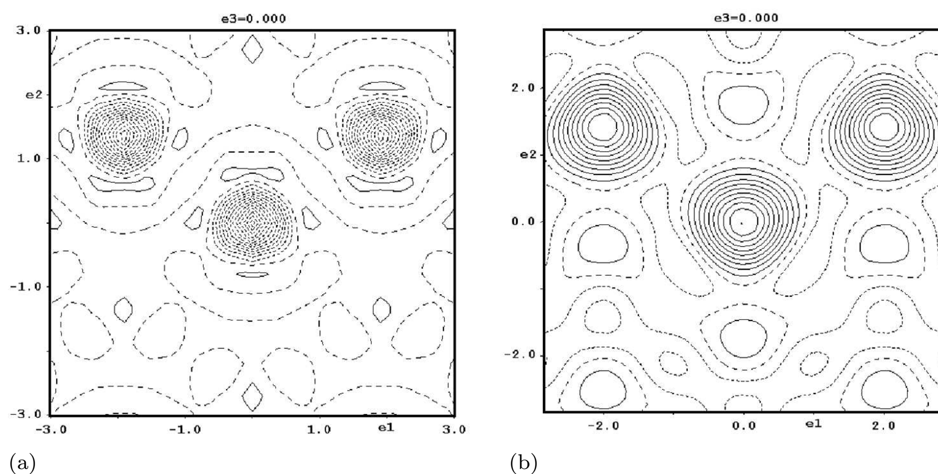

Figure 4. Dynamic multipole deformation map of (**a**) Si on (1 1 0) plane and (**b**) Ge on (1 1 0) plane.

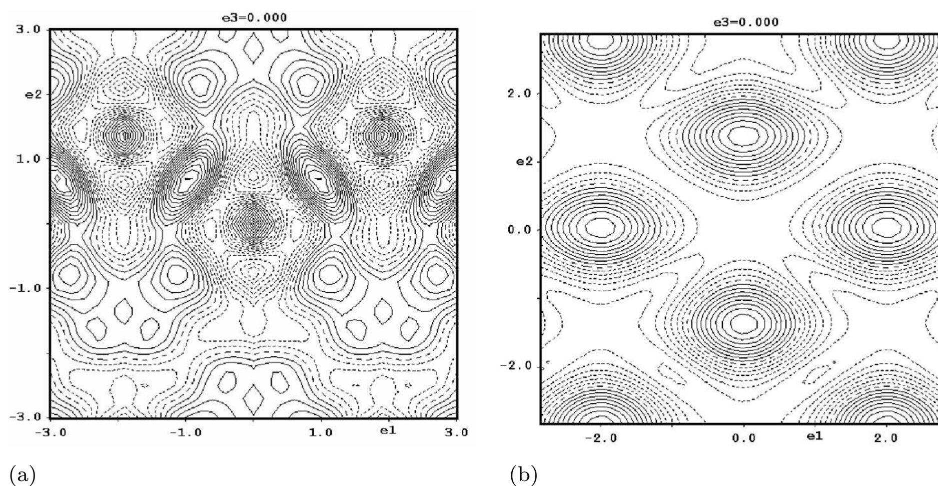

Figure 5. Static multipole deformation (SMD) map of (**a**) Si on (1 1 0) plane and (**b**) Ge on (1 1 0) plane.

been constructed. The results of the MEM refinement have been given in table 5. The results of the 1D analysis have been given in table 6. The 2D electron density contour maps drawn on (1 0 0) plane have been given in figures 6a and 6b for Si and Ge respectively. Figures 7a and 7b represent the 2D electron density maps on the (1 1 0) plane. The local structures using pair distribution function have been given in figure 8 for Si and Ge. The results of the PDF analysis have been given in table 7.

Table 4. Multipole electron densities.

System	Si	Ge
DMD analysis		
Positive Max. (e/Å^3)	0.01	0.09
Negative Max. (e/Å^3)	−0.01	−0.07
SMD analysis		
Positive Max. (e/Å^3)	0.15	2.05
Negative Max. (e/Å^3)	−1.37	−0.51

Table 5. Parameters from the MEM analyses.

Parameter	Si	Ge
Number of cycles	3184	185
Prior density, $\tau(r_i)$ (e/Å^3)	0.087	1.407
Lagrange parameter (λ)	0.010	0.050
R_{MEM} (%)	0.016	0.017
wR_{MEM} (%)	0.005	0.012
Resolution (Å/pixel)	0.085	0.089

Table 6. The one-dimensional electron density of Si and Ge along the three directions in the unit cell.

	Si		Ge	
Direction	Position (Å)	Density (e/Å^3)	Position (Å)	Density (e/Å^3)
[1 0 0]	1.867	0.039	1.238	0.212
[1 1 0]	1.440	0.161	1.251	0.132
[1 1 1]	0.882	0.554	1.227	0.187
[1 1 1] NNM	1.176	0.820	–	–

Table 7. Parameters from pair distribution function.

Parameter	Si	Ge
Refinement range	1.5–30 Å	2–22 Å
Data range	0–30 Å	0–30 Å
Change in R	0.002	0.00016

Table 8. Nearest neighbors in Si and Ge from PDF analysis.

System	Nearest neighbor	Distance (Å)	Observed PDF	Calculated distance*
Si	I	2.18	1.45	2.35
	II	3.88	2.97	3.84
	III	5.24	−3.23	5.43
Ge	I	2.54	3.47	2.44
	II	3.98	7.42	3.99
	III	5.38	−6.50	5.65

*Calculated from Wyckoff [34].

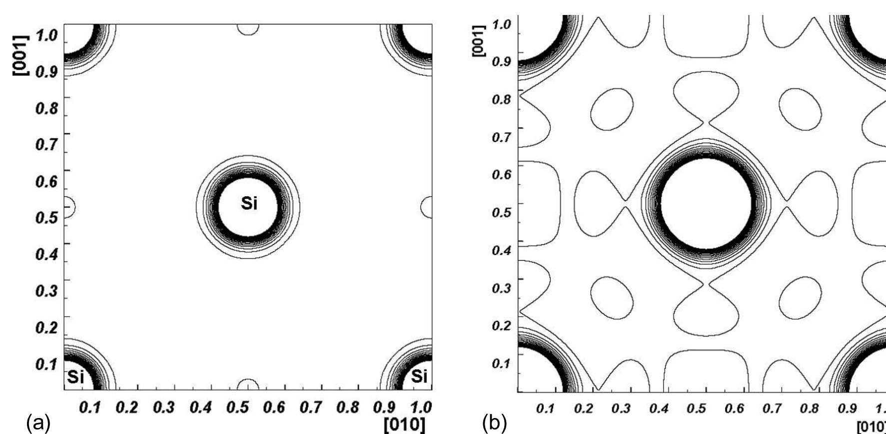

Figure 6. (**a**) MEM electron density distribution of Si on the (1 0 0) plane. Contour range is from 0.4 to 5 e/Å^3. Contour interval is 0.23 e/Å^3. (**b**) MEM electron density distribution of Ge on the (1 0 0) plane. Contour range is from 0 to 2 e/Å^3. Contour interval is 0.1 e/Å^3.

5. Results and discussion

Nowadays numerous crystalline systems are being grown using various techniques for use in application oriented devices. Most of the samples are first analyzed using X-ray powder technique instead of single crystal X-ray diffraction methods, mainly because, the initial sample growth results in polycrystalline samples and most applications need only the samples in powder form or to be coated on some substrate. Moreover, many new crystalline systems cannot be grown as single crystals due to the absence of long-range order. Hence, powder X-ray data should be subjected to maximum possible utility for the characterization of the grown materials. In this context, we have utilized the three novel tools (1) MEM, (2) multipole and (3) PDF method to analyse the X-ray powder data of two

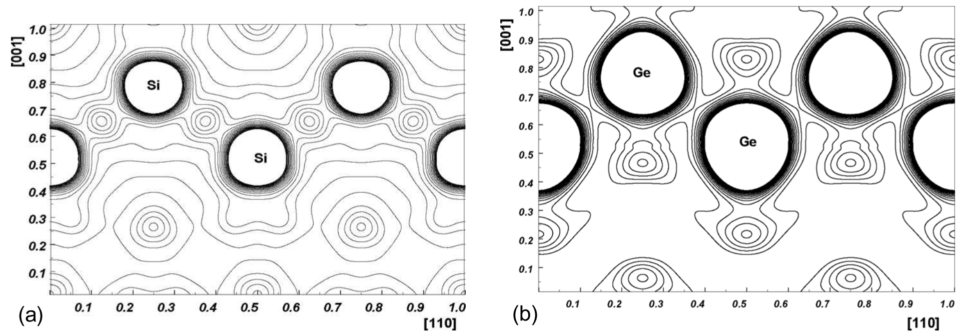

Figure 7. (**a**) MEM electron density distribution of Si on the (1 1 0) plane. Contour range is from 0.05 to 2 e/Å^3. Contour interval is 0.097 e/Å^3. (**b**) MEM electron density distribution of Ge on the (1 1 0) plane. Contour range is from 0.15 to 0.7 e/Å^3. Contour interval is 0.0366 e/Å^3.

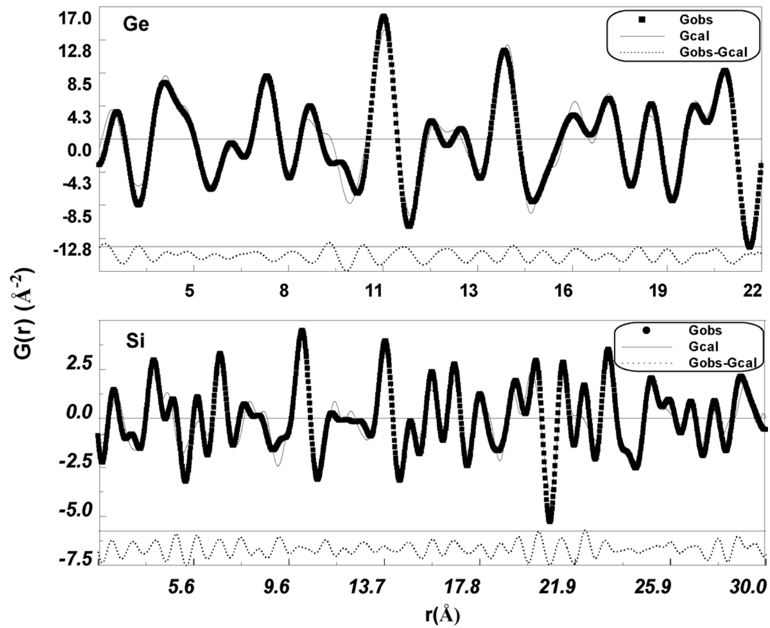

Figure 8. The observed and calculated PDF (pair distribution functions) of Si and Ge.

well-known semiconductors Si and Ge. For any new crystalline system, these methods can be applied to extract the maximum possible information using X-ray data.

The powder data sets of Si and Ge were refined using JANA 2000 [33] using multipole formalism of [17]. The refined structure factors (F_{obs} and F_{cal}) show very small differences with low σ (F_{obs}) values for both the systems as indicated in tables 1 and 2.

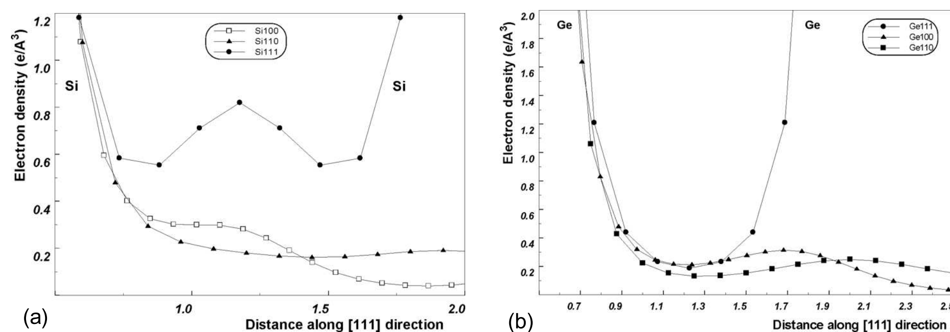

Figure 9. One-dimensional variation of electron density along [1 0 0], [1 1 0] and [1 1 1] directions of (**a**) Si unit cell and (**b**) Ge unit cell.

5.1 *Multipole refinement*

After successful refinement of the structural parameters using JANA 2000 [33], the structure factors were used for the refinement of core, valence and the pseudo-atomic electron occupancies P_{lm} using the formalism proposed by Hansen and Coppens [17] and by the software JANA 2000 [33]. The neutral atom wave functions are taken from Clementi tables [35] and the Slater-type radial functions are used with $n_l = 4, 4, 6, 8$ for $l \leq 4$ according to [17]. The atomic orbitals up to hexadecapole were considered with double zeta function ξ taken as per Lu and Zunger [1]. As described by Dawson [36] and Stewart [37], the multipole deformation functions allowed for the tetrahedral site symmetry of the germanium atom are one octupole (i.e., P_{32-}) and one hexadecapole, the latter being a combination of P_{40} and P_{44} while the other terms vanish due to the site symmetry of the Si and Ge atoms being $\bar{4}3m$. A physically more acceptable argument is that the higher functions effectively account for density in the covalent bond region, which is relatively distant from the nuclear centers. The unit cell electroneutrality condition was imposed during the multipole refinement. The refined parameters show good agreement with the already available literature values and are presented in table 3. The refined κ' parameter of Si shows slight expansion of the valence region as agreed upon by Lu and Zunger [1]. For Ge, there is slight contraction of valence shell as indicated by κ' and k''. The reliability indices and the goodness of fit factors (GoF) confirm the accuracy with which the results are produced and can be credited accordingly.

The structure factors refined after multipole treatment were used for the construction of charge density maps on the (1 0 0) and (1 1 0) planes. The DMD map on the (1 0 0) plane of Si (figure 2a) shows the vibration of outer valence electrons as positive contour lines. The DMD map of Ge (figure 2b) shows perfect spherical inner cores probably due to relatively low thermal vibrations of similar atoms. The SMD map of both Si and Ge (figures 3a and 3b) show clear thermal vibrations of outer regions of the shell. The DMD maps of Si and Ge show (figures 4a and 4b) the nature of bonding on the (1 1 0) plane. The tetrahedral nature of bonding is visible through the shape of the contours. The SMD maps of both systems (figures 5a and 5b) show that the concentration of charges is more in the mid-bond region of Si than in Ge. This fact is reflected in the MEM mid-bond electron densities too.

The effect of the temperature can be distinguished from the convoluted and the deconvoluted forms of thermal contribution to the charge density as dynamic and static multipole deformation maps. These dynamic multipole deformation maps and the static multipole deformation maps clearly visualize that more pronounced deformation in density is at the valence regions than that at the core regions for both the data sets. The maps show pronounced bonding charges. All the maps show less noise and background density confirming the better quality of the maps.

5.2 *MEM refinement*

The clear visualization of bond charge needs the best mathematical tool and the one used for obtaining the charge density is a statistical approach proposed by Collins [19] called maximum entropy method (MEM).

The structure factors refined for structural parameters were used for the MEM procedure to obtain the charge density distribution in a unit cell along with a weak constraint as proposed by Sakata and Sato [5]. Initially, the unit cell is divided into $64 \times 64 \times 64$ pixels and each pixel is uniformly filled with trial density fixed as F_{000}/a_0^3. The structure factors were calculated iteratively while increasing the entropy in charge density in every cycle until the convergence criterion becomes 1 under minimum possible iterations. In our case, it took 3184 and 185 iterations for the data sets of Si and Ge respectively to reach convergence. The residuals given in table 5 show the accuracy of the data and the results can be credited accordingly. The resultant charge density distribution with the resolution given in table 6 can give accurate reliable information about the bonding especially in the valence region which is the prime interest of the study.

The charge density evaluated using MEM refined structure factors of Si is plotted in the two-dimensional space on the (1 0 0) plane in the density range of 0.4 to 5.0 e/Å^3 with the contour interval of 0.23 e/Å^3 (figure 6a). The Ge (1 0 0) MEM map is shown in figure 6b. These figures show the Si and Ge atoms at the corners and the face center of the (1 0 0) plane. They show no unrealistic negative density, which is the characteristic of the MEM procedure. The spherical nature of the atoms and the accumulation of the charges towards the charge center can be visualized from these maps.

The density map plotted upon (1 1 0) plane of Si (figure 7a) also shows the spherical cores of atoms and accumulation of charges towards the centre. The bonding characteristics of the compound can be visualized from this map. It shows the unique bond charges at the centre of two Si atoms. The MEM map on the (1 1 0) plane of Ge is shown in figure 7b. A clear covalent type sharing of charges is seen between two Ge atoms.

A small build-up of charges is observed for Si and this non-nuclear maxima (NNM) is placed exactly at the mid-bond position. This position (see table 6) is almost the same (1.22 Å) for both the data sets which coincides with the tetrahedral covalent radius (sp^3 hybrids) of the atom, i.e., $r_{\rm c}$(Ge) = 1.22 Å [38]. This confirms the fact that the charge accumulated at the mid-bond is because of the quantum mechanical effect of sharing electrons, for the bonding, from the valence orbitals and thus the bonding is confirmed to be covalent. The density measured

at this position is having a magnitude of 0.554 and 0.187 e/Å^3 for Si and Ge respectively. The magnitude of the NNM can be compared with 0.568 e/Å^3 for Si and 1.49 e/Å^3 for diamond [14]. The same qualitative behavior seen in Ge confirms that the system is also covalent as silicon.

The one-dimensional profiles drawn along [1 0 0], [1 1 0] and [1 1 1] directions are plotted (figures 9a and 9b) for both the data sets. These profiles show that the core of the corner Si and Ge atoms ends almost near 0.88 Å and 1.22 Å which is the same that was observed in the bonding direction. The humps and the non-zero densities from there are because of the free spread of the charge densities in the respective directions but the densities assume minimum values at the mid-way between the pair of atoms in that direction. Some important positions and their density values are tabulated in table 6.

5.3 *PDF refinement*

The refined pair distribution function (the Fourier transform of $S(\vec{Q})$, the reduced structure factor) given in figure 8 shows nice matching of observed and calculated PDF's. The PDF refinement can be considered as equivalent to matching the observed X-ray powder data with a model with too little structure parameters. Moreover, high Q data are required for these types of analyses on short-range order and local structure of materials [16,29,30]. In spite of these factors an attempt has been made to use the X-ray powder data for this analysis.

The peaks in the PDF profile correspond to the nearest-neighbor distances and number of atoms as given in table 8. The observed and calculated PDF values have been given in this table along with the observed and calculated I, II and III nearest-neighbor distances. In silicon, the maximum difference in the observed and calculated [34] nearest-neighbor distances turns out to be 0.19 Å, the maximum being 0.04 Å. In Ge, the maximum and minimum differences are 0.27 Å and 0.01 Å. These differences are not too high considering the fact that we have utilized only data with limited Q values. There may be local undulations in the structure of these two systems also which leads to slightly higher neighbor differences in Si and Ge which correspond to lattice repeat distances. The local disorder is expected to affect the repeat distances, because of the diffuse scattering which does not have sharp, single pointed X-ray diffraction phenomenon. Hence, it is reflected only in the local structure analysis tool like PDF. In single crystal analysis, only the Bragg intensities, which are stronger than the diffuse scattering, are taken into account. Hence, one can expect larger deviations in the structural parameters in the local structural analysis like the present one.

6. Conclusion

The precise nature of local and average structure and bonding in Si and Ge has been studied for the first time using three versatile methods, e.g., maximum entropy method, multipole method and pair distribution function, employing powder X-ray data. The bonding and interaction between the neighboring charges is clearly

analyzed. The utility of powder X-ray data sets to extract the maximum possible information from crystalline systems has been the main objective of the present work.

Acknowledgements

One of the authors Syed Ali acknowledges the authorities of Yadava College, Madurai, India, for their encouragement during the course of this research study.

References

[1] Z W Lu and A Zunger, *Acta Crystallogr.* **A48**, 545 (1992)
[2] M Deutsch, *Phys. Rev.* **B45**, 646 (1992)
[3] M A Spackman, *Acta Crystallogr.* **A42**, 271 (1986)
[4] M A Spackman, *Acta Crystallogr.* **A47**, 420 (1991)
[5] M Sakata and M Sato, *Acta Crystallogr.* **A42**, 263 (1990)
[6] M Deutsch, M Hart and S Cummings, *Phys. Rev.* **B42**, 1248 (1990)
[7] S Israel, R Saravanan, N Srinivasan and R K Rajaram, *J. Phys. Chem. Solids* **64**, 43 (2003)
[8] S Israel, R Saravanan and R K Rajaram, *Physica* **B349**, 390 (2004)
[9] D P Kozlenko, A V Belushkin, K Knorr, R L McGreevy, B N Savenko and P Zetterstrom, *Physica* **B299**, 46 (2001)
[10] M Sakata, T Uno and M Takata, *J. Appl. Crystallogr.* **26**, 159 (1993)
[11] R Saravanan, Y Ono, M Ohno, K Isshiki, K Ohno and T Kajitani, *J. Phys. Chem. Solids* **64**, 51 (2003)
[12] R Saravanan and S Israel, *Physica* **B349**, 220 (2004)
[13] K S Syed Ali, R Saravanan, S Israel and R K Rajaram, *Bull. Mater. Sci.* **29**, 107 (2006)
[14] K Yamamoto, Y Takahashi, K Ohshima, F B Okamura and K Yukino, *Acta Crystallogr.* **A52**, 606 (1996)
[15] T Proffen and S J L Billinge, *J. Appl. Crystallogr.* **32**, 572 (1999)
[16] T Egami, *Mater. Trans. Jpn. Inst. Met.* **31(3)**, 163 (1990)
[17] N K Hansen and P Coppens, *Acta Crystallogr.* **A34**, 909 (1978)
[18] T Kajitani, R Saravanan, Y Ono, K Ohno and M Isshiki, *J. Crystal Growth* **229**, 130 (2001)
[19] D M Collins, *Nature (London)* **298**, 49 (1982)
[20] P Debay and H Menki, *Phys. Z.* **31**, 797 (1930)
[21] B E Warren, *X-ray diffraction* (Addison-Wesley, New York, 1969)
[22] D T Bowran and J L Finney, *J. Chem. Phys.* **118**, 8357 (2003)
[23] W Dmowski, B H Toby, T Egami, M A Subramanian, J Gopalakrishan and A W Sleight, *Phys. Rev. Lett.* **61**, 2608 (1988)
[24] T Proffen and S J L Billinge, *J. Appl. Crystallogr.* **32**, 572 (1999)
[25] V Petkov, S J L Billinge, P Larsan, S D Mahanthi, T Vogt, K K Rangen and M G Kanatzidis, *Phys. Rev.* **B65**, 092105 (2002)
[26] B H Toby and T Egami, *Acta Crystallogr.* **A48**, 336 (1992)
[27] P F Peterson, E S Bozin, T Proffen and S J L Billinge, *J. Appl. Crystallogr.* **36**, 53 (2003)

[28] T Egami and S J L Billinge, *Underneath the Bragg peaks: Structural analysis of complex material* (Oxford University Press, London, 2003)
[29] I K Jeong, J Thompson, T H Proffen, A Perez and S J L Billinge, *PDFGetX – A program for obtaining the atomic pair distribution function from X-ray powder diffraction data* (2001)
[30] T Proffen and R Neder, *J. Appl. Crystallogr.* **30**, 171 (1997)
[31] L V Azaroff and M J Buerger, *The powder method in X-ray crystallography* (Mc-Graw Hill Company, New York, 1958)
[32] H M Rietveld, *J. Appl. Crystallogr.* **2**, 65 (1969)
[33] V Petříček, M Dušek and L Palatinus, *JANA 2000, The crystallographic computing system*, Institute of Physics Academy of Sciences of the Czech Republic, Praha, 2000
[34] R W G Wyckoff, *Crystal structures* (Inter-Science Publishers, London, 1963) vol. I
[35] E Clementi and C Roetti, *At. Data Nucl. Data Tables* **14**, 177 (1974)
[36] B Dawson, *Proc. R. Soc. London Ser.* **A298**, 255 (1967)
[37] R F Stewart, *J. Chem. Phys.* **58**, 1668 (1973)
[38] F H Allen, O Kennard, D G Watson, L Brammer, A G Orpen and R Taylor, *J.Chem. Soc. Perkin II* **S1** (1987)
[39] L M Peng, G Ren, S L Dudarev and M Whelan, *Acta Crystallogr.* **A52**, 456 (1996)
[40] R Saravanan, S K Mohanlal and M Nethaji, *Phys. Status Solidi* **B183**, 359 (1994)
[41] R Saravanan, S K Mohanlal and M Nethaji, *Cryst. Res. Technol.* **30**, 115 (1995)